CHEMISTRY
AN ASIAN JOURNAL
www.chemasianj.org

Accepted Article

Title: Ruthenium complexes for catalytic dehydrogenation of hydrazine and transfer hydrogenation reactions

Authors: Mahendra Kumar Awasthi, Deepika Tyagi, Soumyadip Patra, Rohit Kumar Rai, Shaikh M. Mobin, and Sanjay Kumar Singh

To be cited as: *Chem. Asian J.* 10.1002/asia.201800315

Link to VoR: http://dx.doi.org/10.1002/asia.201800315

A Journal of
ACES Asian Chemical Editorial Society

A sister journal of Angewandte Chemie and Chemistry – A European Journal

WILEY-VCH

10.1002/asia.201800315

Ruthenium complexes for catalytic dehydrogenation of hydrazine and transfer hydrogenation reactions

Mahendra Kumar Awasthi[a]†, Deepika Tyagi[a]†, Soumyadip Patra[a], Rohit Kumar Rai[a], Shaikh M. Mobin[a] and Sanjay Kumar Singh*[a]

[a]Discipline of Chemistry, Indian Institute of Technology Indore, Simrol-453552, Indore, India

Abstract

Catalytic dehydrogenation of hydrazine in THF and ethanol was achieved over ruthenium-arene complexes containing N_{imine}-substituted iminopyridine ligands [(η^6-benzene)Ru(κ^2-L)Cl]$^+$ (L = N-hydroxy-iminopyridine, N-methoxy-iminopyridine and N-iso-propyl-iminopyridine). Our findings demonstrated that the catalytic activity for the release of H_2 and N_2 gases, as confirmed by GC-TCD, from hydrazine depends on the temperature (30 ºC – 80 ºC), base (KO^{t}Bu and KOH), and solvents used (THF, ethanol and water). Moreover, the studied complex displayed excellent recyclability for the dehydrogenation of hydrazine (in THF) for six consecutive catalytic runs. ^{1}H NMR and mass spectrometric studies revealed the formation of hydrazine (and phenylhydrazine) coordinated Ru(II)-arene intermediate [(η^6-C_6H_6)Ru(κ^2-L)(RNHNH$_2$)]$^+$ (R = H or Ph), where the coordination of hydrazine to Ru center and subsequent activation of hydrazine (E_a = 57.9 kJmol^{-1}) was expected to be the key step involved in achieving dehydrogenation of hydrazine. Exploring the unique ability to activate hydrazine, these complexes were also employed for the catalytic transfer hydrogenation of styrene and a wide range of nitro substrates in good yields in the presence of hydrazine, further evidenced the involvement of Ru-hydride species during ruthenium catalyzed activation of hydrazine for dehydrogenation and transfer hydrogenation reactions.

†Authors with equal contributions

Keywords: Hydrogen · dehydrogenation · hydrazine · ruthenium · homogeneous catalysis · iminopyridine ligands

10.1002/asia.201800315

Introduction

Hydrazine coordinated transition metal complexes have been receiving huge scientific attention because of the involvement of metal-hydrazine species as important intermediates in several reactions of global importance including nitrogen to ammonia reduction.[1-2] Therefore, such hydrazine coordinated complexes based on Fe, W, Mo, Ir, Ru and others have been extensively explored for diverse applications.[1-27] For instance, Tyler *et al.* X-ray crystallographically characterized a Fe-hydrazine complexes *cis*-[Fe(DMeOPrPE)$_2$(η^2-N_2H_4)][BPh_4]$_2$ {DMeOPrPE = 1,2-bis[bis(methoxypropyl)phosphino]ethane} having η^2-coordinated hydrazine, which further undergoes disproportionation to ammonia in the presence of acid.[9] On the other hand, upon base-promoted deprotonation, such Fe-η^2-N_2H_4 complexes afforded Fe-diazene (Fe-η^2-N_2H_2) complexes, which converted back to Fe-hydrazine complex by treatment with a mild acid.[10-14] Ikariya *et al.* reported Fe complexes containing proton responsive pyrazole pincer ligand, which also facilitated disproportionation of N_2H_4 into nitrogen *via* a diazene intermediate.[15] Ir-based hydrazine complexes [$IrCl_2$(RNHNH_2){P(OEt)$_3$}($AsPh_3$)$_2$]$^+$ (R = H, Me, Ph), synthesized by treating [$IrCl_2$H{P(OEt)$_3$}($AsPh_3$)$_2$] with triflic acid followed by an excess of hydrazine, also undergoes oxidation in the presence of $Pd(OAc)_2$ to form Ir-diazene and Ir-hydride complexes.[16] Very recently, Albertin *et al.* reported Ir-hydrazine complex [(η^5-C_5Me_5)Ir{P(OR)$_3$}(N_2H_4)]$^+$ which also exhibited $Pb(OAc)_4$ assisted oxidation to Ir-diazene complex.[17] Seino and Mizobe *et al.* also reported a (η^5-C_5Me_5)Ir coordinated bis-hydrazine cluster [{(η^5-C_5Me_5)Ir}$_4$(μ_3-S)$_2$(μ_2-H)$_2$(N_2H_4)$_2$]$^{2+}$ having two hydrazine molecules coordinated to a single (η^5-C_5Me_5)Ir moiety connected through the bridging sulphur of the Ir_3 cluster.[18] Analogously, several Ru-hydrazine complexes were also reported, which upon oxidation may form corresponding diazene species,[19a-e] such as, Ru-hydrazine [RuH(N_2H_4)L_4]$^+$ and Ru-bis-hydrazine complexes [Ru(N_2H_4)$_2L_4$]$^{2+}$ (L= P(OEt)$_3$, PPh(OEt)$_2$,

$P(OMe)_3$ resulted in the formation of Ru-diazene complexes upon treatment of $Pb(OAc)_4$ in DCM at -80 ^oC.[20] Similarly, hydrazine coordinated Ru-arene and analogous Os-arene complexes $[(\eta^6\text{-}p\text{-cymene})M\{PPh(OEt)_2\}Cl\ (\kappa^1\text{-}N_2H_4)]^+$ (M = Ru and Os) were also reported to be transformed into corresponding diazene complexes upon treatment with $Pb(OAc)_4$ at -30 °C.[21] In similar fashion, Os-hydrazine complex $[Os(PPh_3)_2\{P(OMe)_3\}(CO)Cl(N_2H_4)]^+$ was also reported to be synthesized by direct treatment of N_2H_4 with $[OsHCl(CO)(PPh_3)_2\{P(OMe)_3\}]$ in the presence of triflic acid, which can be further oxidized to form corresponding Os-diazene complex.[22] Interesting to note, that these important intermediates, including those containing N_2H_4 and N_2H_2 coordinated Fe complexes provided substantial mechanistic insights on the role of these species in several reactions, such as dehydrogenation reactions.

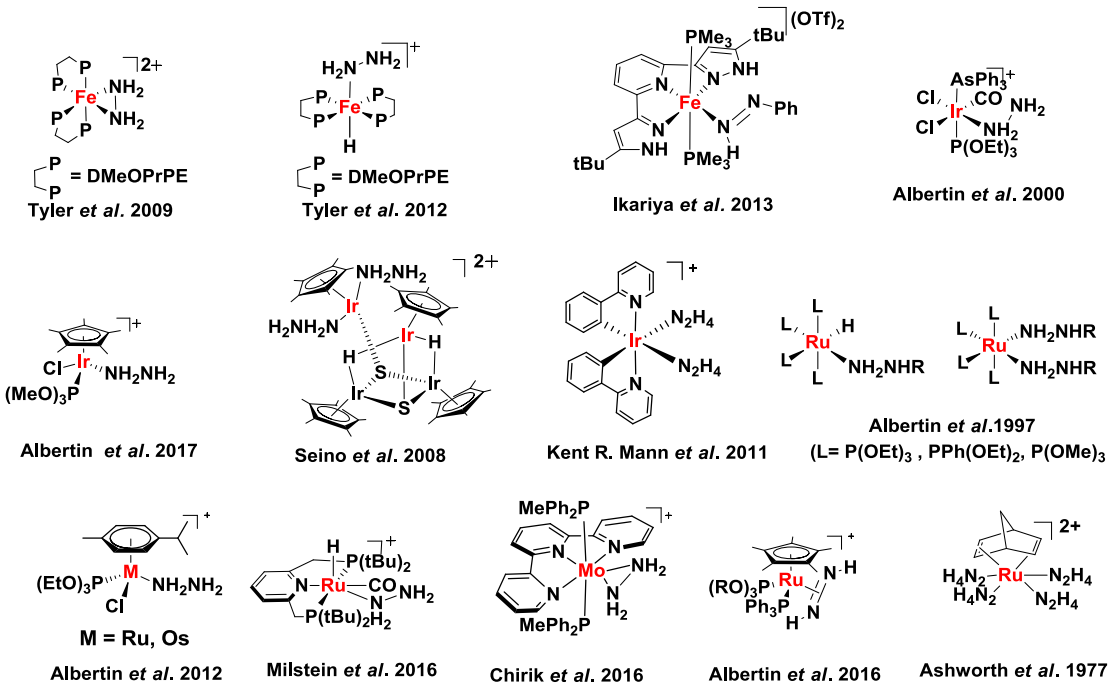

Scheme 1. Various hydrazine coordinated metal complexes – a key step to the activation of hydrazine

In accordance with the above and several other precedent reports on the formation of metal-hydride complex upon treatment of metal-diazene complex with a base, clearly

evidenced a possible pathway for the dehydrogenation of hydrazine.[23-26] For instance, Chirik *et al.* demonstrated the dehydrogenation of hydrazine upon coordination of hydrazine with molybdenum-terpyridine-phosphine in [(^{Ph}Tpy)($PPh_2Me)_2Mo(\kappa^2$-$N_2H_4)$] complex.[26] Field *et al.* also investigated the base-induced dehydrogenation of hydrazine *via* a '*coordination induced activation pathway*' over Ru-tetradentate phosphine complexes, where ligand exerted significant impact on the coordination of hydrazine to Ru (side-on [$RuCl(\kappa^2$-$N_2H_4)(\kappa^3$-$PP_3{}^{ipr})]^+$ or end-on bound hydrazine [$RuCl(\kappa^1$-$N_2H_4)(\kappa^4$-$PP_3{}^{Ph})]^+$) and the reactivity pathway of the resulting complexes.[27] Apart from homogeneous catalysts there are several reports are available in literature for the dehydrogenation of hydrazine using heterogeneous catalyst but exploration of homogeneous complexes for hydrazine activation are particular importance because of several applications.[28,29] However, anhydrous hydrazine is explosive in nature when exposed to a metal catalyst which makes it difficult to handle safely, whereas hydrous hydrazine ($H_2NNH_2{\cdot}H_2O$), which also contains a large amount of hydrogen (7.9 wt %), is much safer and easy to handle.[29]

Therefore, intrigued by aforementioned findings, herein, we report the reactivity of iminopyridine based ruthenium-arene complexes with hydrazine and explored the base assisted catalytic dehydrogenation of hydrazine. ^{1}H NMR and mass spectrometric tools were probed to investigate and evidence the possible interactions between hydrazine and Ru and generation of any possible organometallic intermediates. Further, the application of the ruthenium catalyzed activation of hydrazine was also explored for transfer hydrogenation of nitro substrates and styrene.

Results and discussion

Synthesis and X-ray structure of ruthenium-arene complexes. To perform ruthenium catalyzed dehydrogenation of hydrazine, Ru(II)-arene complexes, [(η^6–

10.1002/asia.201800315

benzene)Ru(N-hydroxy-iminopyridine)Cl]$^+$ (**[Ru]-1**), [(η^6–benzene)Ru(N-methoxy-iminopyridine)Cl]$^+$ (**[Ru]-2**), and [(η^6–benzene)Ru(N-isopropyl-iminopyridine)Cl]$^+$ (**[Ru]-3**), were synthesized following earlier reports (Figure 1a).[30-32] Recrystallization of **[Ru]-2** gave orange colour crystals suitable for single-crystal structure determination (Figure 1b). Complex **[Ru]-2** adopted a *piano-stool* geometry, with bond lengths (Ru-Cl, Ru-N1, and Ru-N2, Ru-C_t) and bond angles (N_{py}-Ru-N_{imine} and $N_{py/imine}$-Ru-Cl) are in the expected range of the analogous ruthenium complexes (see supporting information).[31,32] Moreover, torsion angle N1-C5-C6-N2 (-1.2°) is suggesting the planar arrangement of the bidentate iminopyridine ligand.

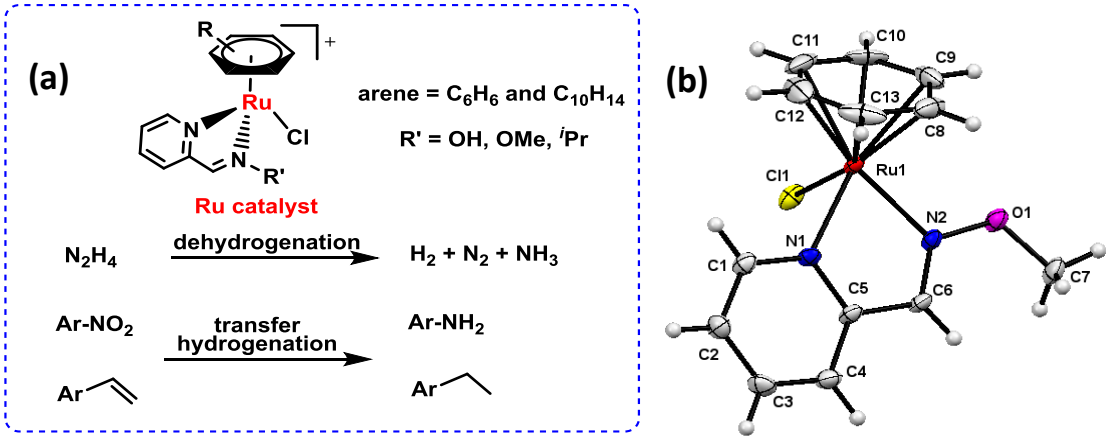

Figure 1. (a) Ruthenium-arene catalyzed dehydrogenation of hydrazine and transfer hydrogenation of nitro substrate and styrene, **(b)** X-ray crystal structure of complex **[Ru]-2** with 30% ellipsoid probability. Counter ion (Cl^-) are omitted for sake of clarity. Selected bond lengths [Å] and angles [deg]: Ru1-Cl1 2.402(11), Ru1-N1 2.098(4), Ru1-N2 2.067(3), N2-C6 1.282(6), Ru1-C_{avg} 2.177, Ru1-C_t 1.444, N1-Ru1-N2 75.80(14), N1-Ru1-Cl1 84.61(10), N2-Ru1-Cl1 87.97(10), N1-C5-C6-N2 -1.2(6).

Ruthenium catalyzed dehydrogenation of hydrazine. At an outset, dehydrogenation of hydrazine monohydrate ($N_2H_4{\cdot}H_2O$) was attempted over **[Ru]-1** complex in water by using base (KOH) at 80 ^oC, where the evolution of gas from the reaction mixture was observed

volumetrically (Table 1, entry 1). Further, an enhancement in TON and a two-fold increment in TOF were observed by performing the experiment in the presence of KO^{t}Bu instead of KOH (Table 1, entry 2). In contrary to water, a significant enhancement in TON was observed for the dehydrogenation reaction performed in ethanol (Table 1, entry 3). Notably, appreciable amount of gas evolution from the hydrazine solution in ethanol was also observed even in the absence of base, but the reaction was observed to be sluggish (Table 1, entry 4). Further in the search of a suitable solvent medium, **[Ru]-1** catalyzed dehydrogenation of hydrazine was performed in THF-methanol (10:1 v/v) at 80 ^{o}C in the presence of different bases KOH, NaOH and KO^{t}Bu, where highest TON and TOF was achieved with KO^{t}Bu (Table 1, entries 5-7). Based on the amount of gas evolved, selectivity for H_2 gas (X) was found to be 0.46.[28-29,33] Moreover, the presence of H_2 in the released gas was also analysed by GC-TCD (Figure S1). Therefore, the overall hydrazine decomposition equation can be expressed which is as follows:

$$N_2H_4 \rightarrow 0.72NH_3 + 0.65N_2 + 0.92H_2 \quad \text{eq. (1)}$$

It should be noted that gas evolution was not observed in the absence of the catalyst (Table 1, entry 8, Figure S2). Furthermore, we performed control experiment under the optimised reaction condition in the absence of hydrazine. There was no traces of gas release was observed during the experiment, inferred that under the optimized reaction condition methanol dehydrogenation does not occurred (Table 1, entry 9, and Figure S2). In addition, analysis of reaction mixture obtained after the reaction does not show any other products, such as CO, CO_2, formate, acetal of formaldehyde, N-methylation of hydrazine. Moreover, using methanol is advantageous, as it increases the solubility of the studied complex in the solution. The above observations inferred that the observed gas release in the presence of hydrazine was due to catalytic dehydrogenation of hydrazine only, and that the presence of both catalysts and hydrazine is important for gas generation. Notably, in THF-methanol, an

10.1002/asia.201800315

enhancement of three- and two-fold, respectively in the TOF was achieved compared to the catalytic dehydrogenation reaction performed in water and ethanol. Further performing the catalytic reaction at lower temperature (< 80 °C), TON and TOF of the catalytic dehydrogenation of hydrazine was significantly decreased (Table 1, entries 10-14). The apparent activation energy (Ea = 57.9 kJmol^{-1}) for the catalytic dehydrogenation of hydrazine over **[Ru]-1** catalyst, as obtained by an Arrhenius plot (Figure 2c (inset) and Figure S3), is in good agreement with other literature findings.[33]

Table 1. Optimization of the reaction condition for the catalytic dehydrogenation of hydrazine over **[Ru]-1** catalyst[a]

Entry	Catalyst	Solvent	Base	T (^{o}C)/ *t* (min.)	Volume of gas (mL)	TON	TOF (h^{-1})
1	**[Ru]-1**	Water	KOH	80/53	8.0	-	-
2	**[Ru]-1**	Water	KO^{t}Bu	80/36	11.0	3.5	5.8
3	**[Ru]-1**	Ethanol	KO^{t}Bu	80/70	35.0	33.0	28.0
4	**[Ru]-1**	Ethanol	-	80/154	25.5	21.0	8.0
5	**[Ru]-1**	**THF-methanol**	**KO^{t}Bu**	**80/40**	**38.5**	**37.0**	**58.5**
6	**[Ru]-1**	THF-methanol	KOH	80/57	36.5	35.0	37.0
7	**[Ru]-1**	THF-methanol	NaOH	80/75	32.0	29.0	23.0
8	-	THF-methanol	KO^{t}Bu	80/120	-	-	-
9*	**[Ru]-1**	THF-methanol	KO^{t}Bu	80/120	-	-	-
10	**[Ru]-1**	THF-methanol	KO^{t}Bu	30/61	8	-	-
11	**[Ru]-1**	THF-methanol	KO^{t}Bu	40/66	9.5	1.64	1.49
12	**[Ru]-1**	THF-methanol	KO^{t}Bu	50/111	16.0	9.5	5.18
13	**[Ru]-1**	THF-methanol	KO^{t}Bu	60/48	38.5	37.0	46.0

10.1002/asia.201800315

14	**[Ru]-1**	THF-methanol	KO^{t}Bu	70/55	38.5	37.0	40.0
15	**[Ru]-2**	THF-methanol	KO^{t}Bu	80/65	36.5	35.0	32.0
16	**[Ru]-3**	THF-methanol	KO^{t}Bu	80/66	33.5	31.0	28.0

[a]Reaction condition: $N_2H_4 \cdot H_2O$ (1.0 mmol), base (20 mol %), catalyst (2.5 mol %), solvent (5.5 mL). THF-methanol (10:1 v/v). *Without hydrazine. TON = $n(H_2)/n(cat)$. TOF = $n(H_2)/\{n(cat) \cdot time\}$.

Further to evaluate the effect of substitutes at N_{imine} of iminopyrdine ligands in the studied ruthenium complexes **[Ru]-1** – **[Ru]-3**, catalytic dehydrogenation of hydrazine was performed under the optimized reaction condition (hydrazine (1.0 mmol), catalyst (2.5 mol%) and KO^{t}Bu (2.5 mol%) in THF-methanol (5.5 mL, 10:1 v/v) at 80 °C) (Table 1, entries 15-16, Figure 2a). Results inferred that among all the studied complexes having different steric and electronic properties, the (η^6-benzene)Ru complex **[Ru]-1** having N_{imine}-OH group outperformed and showed higher TOF (h^{-1}) over those having N_{imine}-OMe and N_{imine}-^{i}Pr substitution (Figure 2b), which can be attributed to the plausible involvement of the hydroxyl group in interaction with hydrazine coordinated with Ru and hence facilitating improved Ru to hydrazine interactions.[34] Notably, the outperforming **[Ru]-1** catalyst exhibited remarkably high recyclability up to six consecutive catalytic runs for the dehydrogenation of hydrazine under the optimized reaction condition (Figure 2d). Moreover, no remarkable change in the catalytic efficacy was observed during the reaction performed in the presence of Hg, suggesting the homogenous nature of the active form of the catalyst (Figure S4).

10.1002/asia.201800315

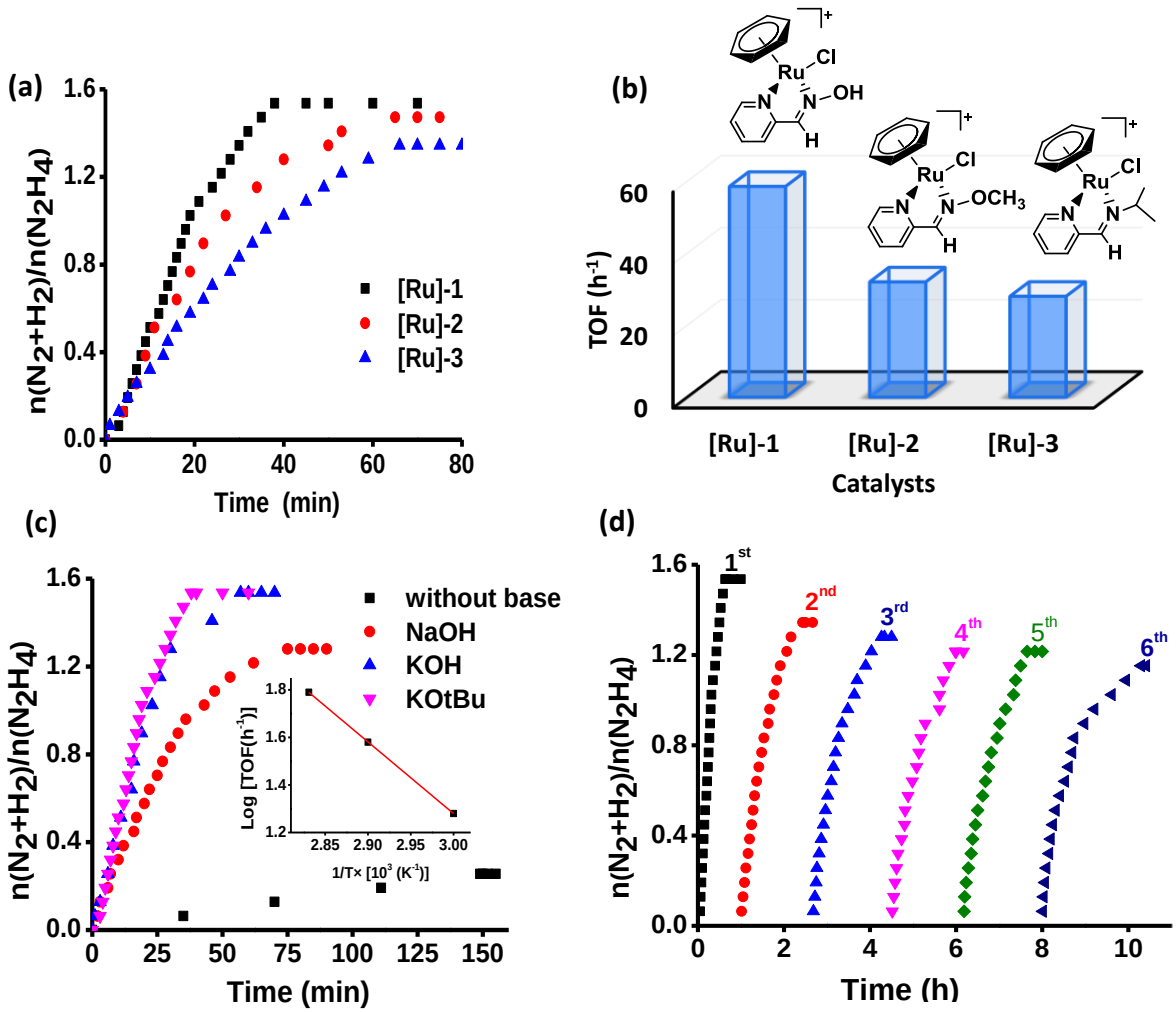

Figure 2. (a-b) Comparative catalytic efficacy (a) amount of gas released *vs* time and (b) TOF (h^{-1}) for the dehydrogenation of hydrazine monohydrate over ruthenium-arene catalysts. (c) Catalytic dehydrogenation of hydrazine monohydrate (1.0 mmol) over **[Ru]-1** catalyst (2.5 mol%) in the presence and absence of base (20 mol%) (inset), Arrhenius plot for the dehydrogenation of hydrazine monohydrate over **[Ru]-1** catalyst at 30, 40, 60 and 80 °C to estimate the activation energy (R^2 = 0.991). (d) Recyclability experiments for the catalytic dehydrogenation of hydrazine monohydrate over **[Ru]-1** catalyst. Reaction condition: hydrazine monohydrate (1.0 mmol) over various ruthenium catalysts (2.5 mol%) in the presence of KO^{t}Bu (20 mol%) in THF-methanol (5.5 mL, 10:1 v/v) at 80 °C.

To further investigate the role of Ru-catalyst in the catalytic dehydrogenation of hydrazine, several controlled and catalytic experiments were performed to identify the crucial

10.1002/asia.201800315

organometallic intermediates which might be generated during the reaction due to the possible interactions between Ru-catalyst and hydrazine. In this context, control experiment performed using **[Ru]-1** catalyst in D_2O with an excess of hydrazine added, showed a peak at m/z 333.0 in mass spectra corresponding to the hydrazine coordinated Ru-species, **[Ru]-1A**. Coordination of hydrazine to ruthenium was further evidenced by ^{1}H NMR, where an upfield shifting in the peaks corresponding to iminopyridine ligand in **[Ru]-1** complex was observed (Figure S5). Further, an analogous behaviour in ^{1}H NMR was also observed when an excess of hydrazine was added in a solution of **[Ru]-1** complex in CD_3OD, and the corresponding mass data also showed m/z value of 333.0 corresponding to the **[Ru]-1A** species (Figure S6). Moreover, mass spectral analysis of the reaction aliquot during the catalytic reaction condition also evidenced the formation of a hydrazine coordinated ruthenium species (Figure S7). The catalysts **[Ru-1]** having N–OH substitution outperformed over **[Ru]-2** and **[Ru]-3** having N-OMe and N-^{i}Pr substitutions respectively, possibly because of the presence of protic group N–OH. In the presence of a base, the protic group N-OH deprotonated and thereby stabilised a hydrazine coordinated monocationic ruthenium species [(η^6–benzene)Ru(N-hydroxy-iminopyridine)N_2H_4]$^+$ (**[Ru]-1A**), which was well characterised by mass (m/z 333.0) and NMR (Figure S5-S7). Analogously, **[Ru]-2** and **[Ru]-3** complexes also showed the formation of corresponding hydrazine coordinated ruthenium species and due to lack of protic group these ruthenium hydrazine species are dicataionc species **[Ru]-2A** (m/z 174.0) and **[Ru]-3A** (m/z 180.0) (Figure 3 and Figure S8-S9).

10.1002/asia.201800315

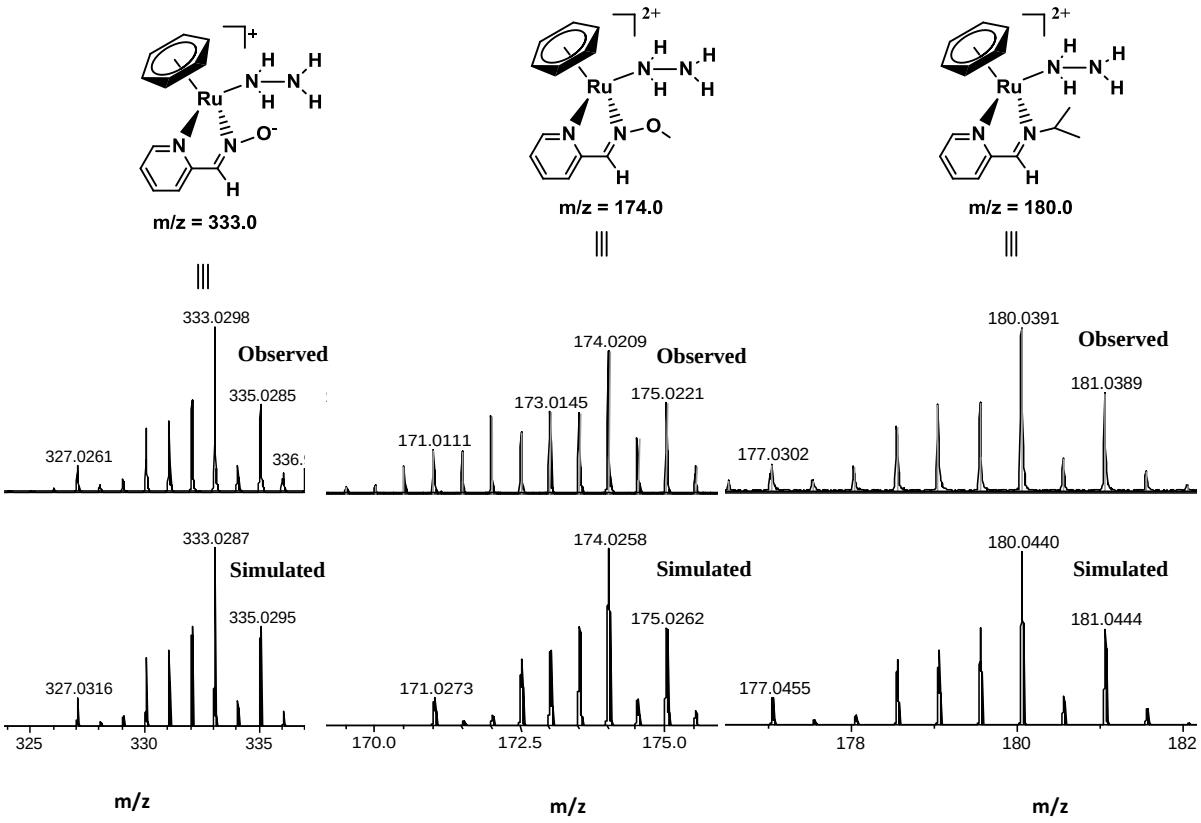

Figure 3. Mass spectral analysis for the hydrazine coordinated ruthenium species, **[Ru]-1A**, **[Ru]-2A** and **[Ru]-3A**, obtained by the addition of hydrazine to an aqueous solution of the corresponding complexes **[Ru]-1**, **[Ru]-2** and **[Ru]-3**, respectively.

Moreover, the addition of hydrazine to a pale yellow solution of **[Ru]-1** in water resulted in an intense wine-red solution, suggested the formation of ruthenium-hydrazine species. The significant shift in the ^{1}H NMR spectra and the presence of a mass peak at m/z 333.0 corresponds to the **[Ru]-1A** species clearly evidenced the formation of ruthenium-hydrazine species. Further addition of an excess of dil. HCl in the above wine-red solution immediately resulted in the regeneration of pale yellow solution, thus straight forward evidenced the recovery of **[Ru]-1**, which was also supported by the reappearance of m/z peak at 337.0 (in the mass spectral analysis of the pale yellow solution) corresponding to the **[Ru]-1** catalyst (Figure S10).

Therefore, mass and ^{1}H NMR spectral results clearly evidenced the coordination of hydrazine to Ru center is a crucial step for the activation of hydrazine, which further transformed to Ru-H species via a well-established diazene intermediate. The temperature dependent ^{1}H NMR and corresponding mass analysis under the catalytic reaction condition also inferred the appearance of a ruthenium-hydrazine species with the increase in the reaction temperature (30-60 °C) (Figures S11 and S12). Analogous to hydrazine coordinated ruthenium species, phenylhydrazine also coordinated with the ruthenium metal, and such phenylhydrazine coordinated ruthenium species [(η^6–benzene)Ru(N-hydroxy-iminopyridine){$N_2H_3(C_6H_5)$}]$^+$ (m/z 409.0) were analysed by ^{1}H NMR and mass. (Figure S13-S14). (Figure S13 and Figure S14). Whilst we were unable to observe the Ru-H and Ru-diazene intermediates during our investigations, presumably because of the lower stability of these species in the reaction medium, such species are expected to be involved in the dehydrogenation of hydrazine. Notably, X-ray structure of analogous ruthenium-diazene species [(η^5-Cp*)Ru(κ^2-HN=NH){$P(OEt)_3$}$_2$]$^+$ was previously reported by Albertin *et al.*.[4a] Also, Hillhouse *et al.* demonstrated the formation of metal-diazene and metal-hydride species from rhenium-hydrazine complexes.[5] In this regard, treating 4-methoxystyrene with hydrazine over **[Ru]-1** catalyst resulted in the formation of 1-ethyl-4-metoxy benzene in water-ethanol at 80 ºC, suggesting the possible involvement of ruthenium-hydride species during the transfer hydrogenation via an ruthenium catalyzed activation of hydrazine (Figure S15). In a recent report, Milstein *et al.* also demonstrated the crucial role of a hydrazine-coordinated Ru intermediate species [(^{t}BuPNP)Ru(CO)(H)(N_2H_4)]$^+$ during a Ru-pincer complex catalyzed dehydrogenative coupling of alcohols with hydrazine with the release of H_2 gas.[25] Similar activation of hydrazine, by weakening of N-H bond of hydrazine upon coordination of hydrazine with molybdenum-terpyridine-phosphine has also been demonstrated.[26] It has been observed that such metal hydrazine complexation lower the

10.1002/asia.201800315

nitrogen-hydrogen bond dissociation free energy (34.6 kcal mol^{-1}) and hence enable H_2 evolution and hydrogenation of styrene.[26] Analogous Ru-hydride and Ru-diazene intermediates were also observed during dehydrogenation of hydrazine over Ru-tetradentate phosphine complexes *via* a 'coordination induced activation pathway'.[27] Based on the above findings and spectral data (mass and ^{1}H NMR) we proposed a plausible general reaction pathway for the hydrazine activation with ruthenium complexes shown in the Scheme 2. Moreover, the formation of hydrazine coordinated ruthenium species for all the complexes **[Ru]-1**, **[Ru]-2** and **[Ru]-3**, suggesting that these complexes probably follow an analogous hydrazine dehydrogenation pathway, as illustrated in Scheme 2.

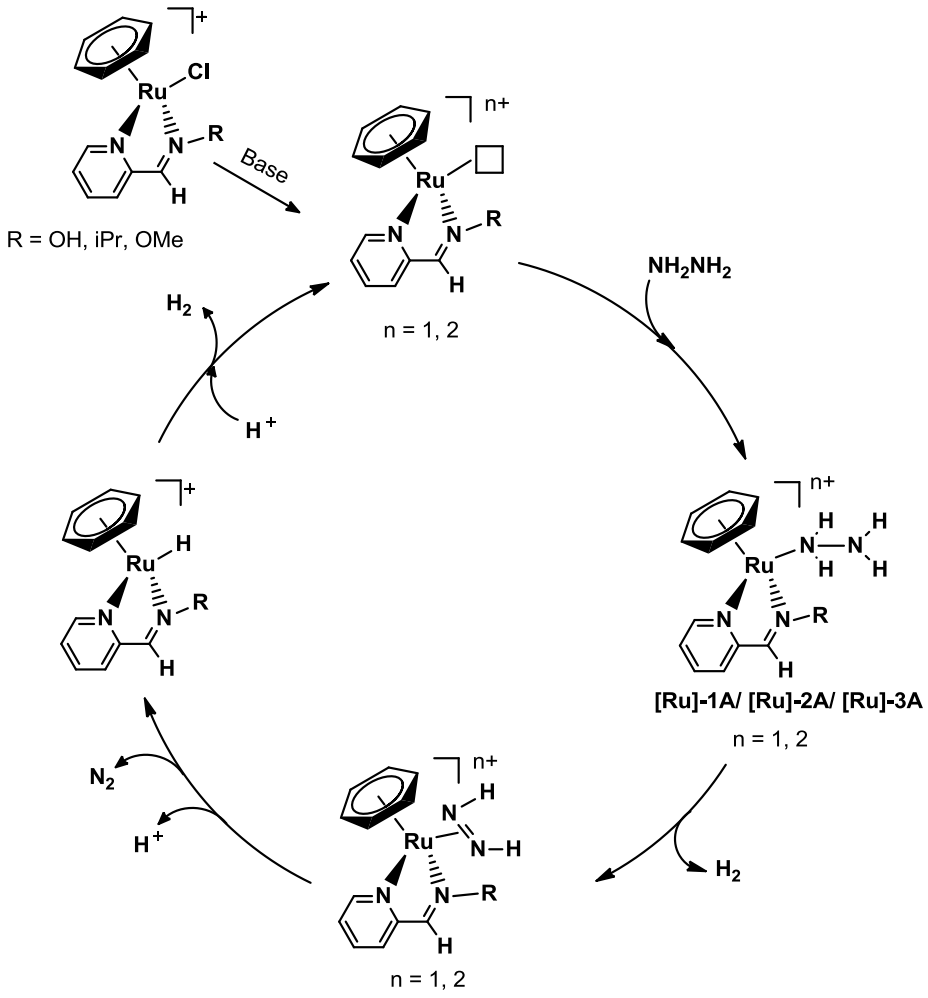

Scheme 2. Plausible reaction pathway for the dehydrogenation of hydrazine over the studied ruthenium catalysts.

Further, the transfer hydrogenation of 4-chloronitrobenzene (**1a**) was also investigated over **[Ru]-1** catalyst in the presence of hydrazine at 80 ºC, which led to the formation of 4-chloroaniline (**1b**) in high yield (Table 2 and Table S4-S5). Notably, reaction could not proceed in the absence of either the catalyst or hydrazine, suggesting the active role of the catalyst in the activation of hydrazine and possibly generation of the most crucial Ru-hydride intermediate to facilitate the catalytic transfer hydrogenation reaction (Scheme S1).[31a] Further, we monitored the reaction progress and identified different possible intermediates by using UV-vis and ^{1}H NMR (Figure S16-S17). The UV-vis spectrum showed the formation of a 4-chloronitrosobenzene intermediate (276 nm) after 2 h reaction progress, but we could not find any absorbance for other possible intermediate (Figure S16). However, in ^{1}H NMR spectra we were able to identify different intermediates, such as phenylhydroxylamine, nitrosobenzene, and azoxybenzene, formed during nitrobenzene reduction (Figure S17).[35] The above results illustrated a step wise hydrogen transfer to nitro group of nitrobenzene, which led to the formation of different intermediate phenylhydroxylamine, nitrosobenzene, and azoxybenzene, which were further transformed to aniline (Scheme S1). Moreover, in accordance to the dehydrogenation process, complexes other than **[Ru]-1** were also found to be poorly active for transfer hydrogenation of **1a**. Worthy to mention, that the catalytic transfer hydrogenation of nitro substrates was found to be a base free transformation. Along with the efficient transformation of nitrobenzene (**2a**) to aniline (**2b**), a wide range of other nitro substrates were also employed for the transfer hydrogenation reaction over **[Ru]-1** catalyst. Nitro substrates with electron withdrawing substituents such as 4-chloronitrobenzene (**1a**), 3-chloronitrobenzene (**3a**) and 4-bromonitrobenzene (**4a**) showed excellent conversion to afford corresponding amines (**1b**, **3b**, **4b**) (Table 2). Nitro substrates with electron donating groups, such as 4-nitrobenzylalcohol (**5a**), 4-methylnitrobenzene (**6a**), 3-methylnitrobenzene (7**a**) and 4-methoxynitrobenzene (**8a**) were also transformed efficiently to corresponding

10.1002/asia.201800315

amines (**5b-8b)** in excellent yields (Table 2). More interestingly, chemoselective transfer hydrogenation of nitro-groups in 4-nitrobenzonitrile (**10a**) and 4-nitrobenzaldehyde (**11a**) to corresponding amines, 4-aminobenzonitrile (**10b**) and 4-aminobenzaldehyde (**11b**) with 97% and 80% yield respectively was also achieved (Table 2). 2-nitrobiphenyl (**12a**) and 8-nitroquinoline (**13a**) were also efficiently converted into the corresponding amines, **12b** and **13**b with 96% and 90% yield respectively (Table 2).

Table 2. Functional group tolerance for the catalytic transfer hydrogenation of nitro substrate[a]

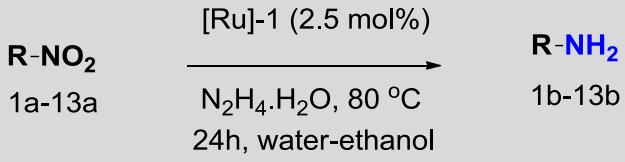

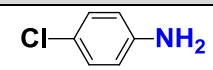
(1b)
Conv. >99 (97)[c][d]

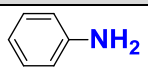
(2b)
Conv. >99 (96)[e]

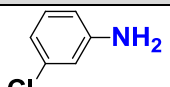
(3b)
Conv. >99 (95)[e]

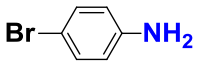
(4b)
Conv. >99 (96)[f]

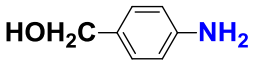
(5b)
Conv. >99 (96)[f]

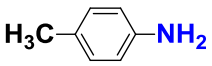
(6b)
Conv. >99 (96)[f]

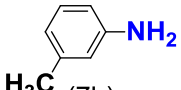
(7b)
Conv. >99 (94)[f]

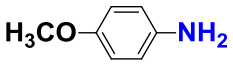
(8b)
Conv. >99 (97)[f]

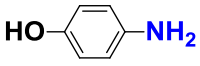
(9b)
Conv. >60 (55)[f]

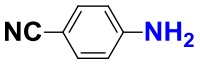
(10b)
Conv. >99 (97)[e]

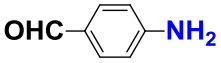
(11b)
Conv. >99(80)[e]

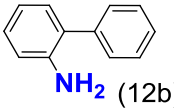
(12b)
Conv. >99 (96)[f]

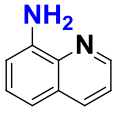
(13b)
Conv. >99 (90)[f]

[a]Reaction conditions: nitro substrate (1 mmol), **[Ru]-1** (2.5 mol%), $N_2H_4 \cdot H_2O$ (2 - 10 equiv.), ethanol-water (5 mL, 1:1 v/v), conversion determined by ^1H NMR, isolated yields (%) are given in parenthesis, [c] 6h, [d] 2 equiv. $N_2H_4 \cdot H_2O$, [e] 5 equiv. $N_2H_4 \cdot H_2O$, [f] 10 equiv. $N_2H_4 \cdot H_2O$

Conclusions

We demonstrated catalytic dehydrogenation of hydrazine over ruthenium-arene catalysts containing N-substituted iminopyridine ligands at 80 ºC in ethanol and THF-methanol in the presence of a base. Our findings suggested a ligand-accelerated dehydrogenation of hydrazine, where the ruthenium complex **[Ru]-1** containing N-hydroxyiminopyridine ligand outperformed over others. The evolved gas was analysed by GC-TCD. Our experimental findings along with ^{1}H NMR and mass studies evidenced the presence of a hydrazine coordinated ruthenium species. These observations suggesting a possible coordination assisted activation of hydrazine N-H bond over ruthenium catalyst to release hydrogen gas *via* a Ru-hydride species. Subsequently, the involvement of Ru-hydride species was further confirmed by achieving efficient transfer hydrogenation of nitro substrates and styrene in good yields over **[Ru]-1** catalyst in the presence of hydrazine. Further efforts to explore more into the mechanistic aspect of the ruthenium catalyzed dehydrogenation of hydrazine are underway.

Experimental Section

Materials. All experiments were carried out using the chemicals of higher purity purchased from Sigma Aldrich, TCI and Alfa Aesar unless otherwise specified, except the ligands and complexes prepared by us. Ru(II)-arene complexes were synthesized according to previous reports using, Ru(II)-arene precursors, $[\{(\eta^6\text{-benzene})RuCl_2\}_2]$.[36]

Instrumentation. ^{1}H NMR (400 MHz) spectra were recorded at 298 K using $CDCl_3$, D_2O and DMSO-d_6 as a solvent on a Bruker Avance 400 spectrometer using tetramethylsilane (TMS) as an external standard. Chemical shifts (in ppm) are relative to the center of the singlet at 7.26 ppm for $CDCl_3$, 4.75 ppm for D_2O and 2.49 for DMSO-d_6 in ^{1}H NMR respectively. Coupling constant (J) values are reported in hertz (Hz), and the splitting patterns

are designated as follows: s (singlet); d (doublet); t (triplet); m (multiplet); br. (broad). ESI-mass spectra (Positive mode) were recorded on a micrOTF-Q II mass spectrometer. UV-visible absorption spectra were recorded on a Carry-60 UV-visible Spectrophotometer using 10 mm quartz cuvettes. GC−TCD analysis was performed on a Shimadzu GCMS-QP2010 Ultra and GC-2010 Plus system in EI (electron impact) mode using RT-Msieve 5A column.

Single crystal X-ray diffraction Studies. Single crystal X-ray structure studies of complex [**Ru]-2**, from the suitable crystals grown by slow diffusion of diethyl ether into the methanol solution of complex [**Ru]-2** was accomplished on a CCD Agilent Technologies (Oxford Diffraction) SUPERNOVA diffractometer. Crystal data for complexes [**Ru]-2** was collected at 293(2) by the standard 'phi-omega' scan techniques and were scaled and reduced using CrysAlisPro RED software, using graphite-monochromated Cu Kα radiation (λ = 1.5418 Å) based diffraction. The extracted data was evaluated using the CrysAlisPro CCD software. The structures were solved by direct methods using SHELXS-97, and refined by full matrix least-squares with SHELXL-97, refining on F^2.[37] Direct methods determined the positions of all the atoms. All non-hydrogen atoms were refined anisotropically. The remaining hydrogen atoms were placed in geometrically constrained positions and refined with isotropic temperature factors, generally 1.2*Ueq* of their parent atoms. The CCDC number 1535290 contains the supplementary crystallographic data for [**Ru]-2**. The data is freely available at www.ccdc.cam.ac.uk (or can be procured from the Cambridge Crystallographic Data Centre, 12 Union Road, Cambridge CB21 EZ, UK; Fax: (+44) 1223-336-033; or deposit@ccdc.cam.ac.uk).

Catalytic dehydrogenation of hydrazine over ruthenium catalysts. A two neck round bottom flask attached to a condenser and equipped with a magnetic bar was charged

with ruthenium catalyst (2.5 mol %), potassium tertiary butaoxide (20 mol%), THF-methanol (5.5 mL, 10:1 v/v). The resulting solution was heated at 80 °C for 15 minute until the colour changes from yellow to dark brown. Now addition of hydrazine in the solution resulted in a colour change from dark brown to the red brown. The gas released during the reaction was passed through a hydrochloric acid solution (2.0 M) before measured volumetrically by a water displacement method. Later, the presence of hydrogen in the generated gas was confirmed by GC-TCD.

Mass spectral studies to identify the hydrazine-coordinated ruthenium species [Ru]-1A. In a separate experiment, complex **[Ru]-1** (0.020 mg, 0.05 mmol) and an excess of hydrazine monohydrate (25 µL, 0.5 mmol) were mixed in 1 mL solution of H_2O. The reaction mixture was stirred at room temperature for 5 minute, where a colour change from yellow to wine-red was observed. An aliquot of the reaction mixture was analysed by mass spectrometry to identify a hydrazine coordinated Ru(II)-arene species ([**Ru]-1A**) at m/z 333.0. Similarly, under the catalytic reaction condition, aliquot from the crude reaction mixture was taken out to analyse by mass spectrometry and similar intermediate species [**Ru]-1A** was observed.

NMR spectral studies to identify the hydrazine-coordinated ruthenium species [Ru]-1A. To confirm the identity of a plausible hydrazine coordinated species [**Ru]-1A** by ^{1}H NMR, complex [**Ru]-1** (0.010 g) in D_2O (500 µL) and hydrazine monohydrate (12.5 µL) were taken into an NMR tube and analysed by ^{1}H NMR.

Recyclability experiments. For the recyclability experiment after every cycle the 20 mol% potassium tertiary butoxide added along with 1 mmol of hydrazine and gas was produced measured by volumetrically.

Catalytic transfer hydrogenation of nitro substrates. Ru(II)-arene complex [**Ru]-1** (0.0093 g, 2.5 mol%) was dissolved in water-ethanol mixture (5.0 mL, 1:1 v/v), followed by the addition of nitro substrate (1 mmol) and hydrazine monohydrate (2 – 10 equiv.) in graduated test tube. The reaction mixture was led to stir at 80 °C for desired reaction time in open air condition. Progress of reaction was monitored by thin layer chromatography (TLC) to observe the complete conversion of substrate. After complete reaction, the reaction mixture was extracted with ethyl acetate (3 × 10 mL). The combined organic layer was dried over sodium sulfate, and solvents were removed *in vacuo* to afford the desired product. All the products were identified by ^{1}H NMR spectroscopy.

Acknowledgements

Authors gratefully acknowledge the financial support from IIT Indore, SERB-DST and CSIR. Discipline of Chemistry, IIT Indore and SIC, IIT Indore are acknowledged for laboratory and instrumentation facilities. M.K.A. thanks MHRD and INSPIRE-DST for his fellowship. D.T. thanks UGC-CSIR for her SRF grant. S.P. and R.K.R. thanks MHRD and IIT Indore, respectively for their fellowships.

References

[1] B. M. Barney, D. Lukoyanov, T.-C. Yang, D. R. Dean, B. M. Hoffman, L. C. Seefeldt, *Proc. Natl. Acad. Sci. USA*. **2006**, *103*, 17113.

[2] B. M. Barney, H.-I. Lee, P. C. D. Santos, B. M. Hoffman, D. R. Dean, L. C. Seefeldt, *Dalton Trans*. **2006**, 2277-2284.

[3] G. Albertin, S. Antoniutti, A. Botter, J. Castro, *Inorg. Chem.* **2015**, *54*, 2091-2093.

[4] (a) G. Albertin, S. Antoniutti, M. Bortoluzzi, A. Botter, J. Castro, *Inorg. Chem.* **2016**, *55*, 5592-5602; (b) T. V. Ashworth, E. Singleton, J. J. Hough, *J. Chem. Soc., Dalton Trans.* **1977**, 1809-1815.

[5] T.-Y. Cbeng, J. C. Peters, G. L. Hillhouse, *J. Am. Chem. Soc*. **1994**, *116*, 204-207.

[6] (a) B. Wu, K. M. Gramigna, M. W. Bezpalko, B. M. Foxman, C. M. Thomas, *Inorg. Chem*. **2015**, *54*, 10909-10917; (b) H.-P. Jia, E. Goure, X. S.-Monfort, J. L. Castelbou, C. Chow, M. Taoufik, O. Eisenstein, E. A. Quadrelli, *Inorg. Chem*. **2015**, *54*, 11648-11659.

[7] C. T. Saouma, C. E. Moore, A. L. Rheingold, J. C. Peters, *Inorg. Chem*. **2011**, *50*, 11285-11287.

[8] K. R. Schwartz, K. R. Mann, *Inorg. Chem*. **2011**, *50*, 12477-12485.

[9] J. L. Crossland, L. N. Zakharov, D. R. Tyler, *Inorg. Chem*. **2007**, *46*, 10476-10478.

[10] L. D. Field, H. L. Li, A. M. Magill, *Inorg. Chem*. **2009**, *48*, 5-7.

[11] J. L. Crossland, C. G. Balesdent, D. R. Tyler, *Dalton Trans*. **2009**, 4420-4422.

[12] D. Sellmann, H. Friedrich, F. Knoch, M. Moll, *Z. Naturforsch*. **1993**, *48b*, 76-88.

[13] D. Sellman, A. Hennige, *Angew*. *Chem. In. Ed. Engl*. **1997**, *36*, 276-278.

[14] J. L. Crossland, C. G. Balesdent, D. R. Tyler, *Inorg. Chem*. **2012**, *51*, 439-445.

[15] K. Umehara, S. Kuwata, T. Ikariya, *J. Am. Chem. Soc*. **2013**, *135*, 6754-6757.

[16] G. Albertin, S. Antoniutti, E. Bordignon, F. Menegazzo, *J. Chem. Soc*. *Dalton Trans*. **2000**, 1181-1189.

[17] G. Albertin, S. Antoniutti, M. Bortoluzzi, J. Castro, *Inorg. Chim. Acta*. **2018**, *470*, 139-148.

[18] H. Seino, A. Saito, H. Kajitani, Y. Mizobe, *Organometallics* **2008,** *27*, 1275-1289.

[19] (a) M. Kawano, C. Hoshino, K. Matsumoto, *Inorg. Chem*. **1992**, *31*, 5158-5159; (b) J. Chatt, G. J. Leigh, R. J. Paske, *J. Chem. Soc. A* **1969**, 854-859; (c) T. V. Ashworth, E. Singleton, J. J. Hough, *J. Chem. Soc., Dalton Trans*. **1977**, 1809-1815; (d) G. Albertin, S. Antoniutti, M. Bortoluzzi, J. C.-Fojo, S. G.-Fontan, *Inorg. Chem*. **2004**,

43, 4511-4522; (e) Q.-F. Zhang, H. Zheng, W.-Y. Wong, W.-T. Wong, W.-H. Leung, *Inorg. Chem*. **2000**, *39*, 5255-5264.

[20] G. Albertin, S. Antoniutti, A. Bacchi, E. Bordignon, P. M. Dolcetti and G. Pelizzi, *J. Chem. Soc., Dalton Trans*. **1997**, 4435-4444.

[21] G. Albertin, S. Antoniutti, J. Castro, *J. Organomet. Chem*. **2012**, 697, 6-14.

[22] G. Albertin, S. Antoniutti, L. Bonaldo, A. Botter, J. Castro, *Inorg. Chem*. **2013**, *52*, 2870-2879.

[23] T.-Y. Cbeng, J. C. Peters, G. L. Hillhouse, *J. Am. Chem. Soc.* **1994**, *116*, 204-207.

[24] G. Albertin, S. Antoniutti, E. Bordignon, F. Menegazzo, *J. Chem. Soc., Dalton Trans*. **2000**, 1181-1189.

[25] J. O. Bauer, G. Leitus, Y. B.-David, D. Milstein, *ACS Catal.* **2016**, *6*, 8415-8419.

[26] M. J. Bezdek, S. Guo, P. J. Chirik, *Science* **2016**, *354*, 730-733.

[27] L. D. Field, H. L. Li, S. J. Dalgarno, R. D. McIntosh, *Inorg. Chem*. **2013**, *52*, 1570-1583.

[28] (a) S. Lee, C. Fan, T. Wu, S. L. Anderson, *J. Phys. Chem. B*, **2005**, *109*, 381; (b) J. Song, R. Ran, Z. Shao, *Int. J. Hydrogen Energy*, **2010**, *35*, 7919; (c) N. Cao, L. Yang, C. Du, J. Su, W. Luo, G. Cheng, *J. Mater. Chem. A*, **2014**, 2, *14344*.

[29] (a) S. K. Singh, X.-B. Zhang, Q. Xu *J. Am. Chem. Soc*. **2009**, *131*, 9894-9895; (b) S. K. Singh, Q. Xu *Catal. Sci. Technol***. 2013**, *3*, 1889-1900, (c) A. K. Singh, M. Yadav, K. Aranishi, Q. Xu, *Int. J. Hydrogen Energy* **2012**, *37*, 18915.

[30] T. S. Ribeiro, A. Prates, S. R. Alves, J. J. Oliveira-Silva, C. A. S. Riehl, J. D. Figueroa Villar, *J. Braz. Chem. Soc.* **2012**, *23*, 1216-1225.

[31] (a) J. M. Gichumbi, H. B. Friedrich, B. Omondi, *Transition Met. Chem.* **2016**, *41*, 867-877; (b) J. M. Gichumbi, H. B. Friedrich, B. Omondi, *J. Organomet. Chem.* **2016**, *808*, 87-96.

[32] D. Tyagi, R. K. Rai, S. M. Mobin, S. K. Singh, *Asian J. Org. Chem*. **2017**, *6*, 1647-1658.

[33] P. Zhao, N. Cao, J. Su, W. Luo, G. Cheng, *ACS Sustainable Chem. Eng.* **2015**, *3*, 1086-1093.

[34] I. Nieto, M. S. Livings, J. B. Sacci, L. E. Reuther, M. Zeller, E. T. Papish, *Organometallics* **2011**, *30*, 6339-6342.

[35] R. K. Rai, A. Mahata, S. Mukhopadhyay, S. Gupta, P.-Z. Li, K. T. Nguyen, Y. Zhao, B. Pathak, S. K. Singh, *Inorg. Chem*. **2014**, *53*, 2904-2909.

[36] (a) M. A. Bennett, T.-N. Huang, T. W. Matheson, A. K. Smith, *Inorg. Synth.* **1982**, *21*, 74-78; (b) R A. Zelonka, M. C. Baird, *Can. J. Chem.* **1972**, *50*, 3063-3072.

[37] G. M. Sheldrick, *Acta Crystallogr., Sect. A: Found. Crystallogr.* **2008**, *A64*, 112-122.

10.1002/asia.201800315

Table of Content

Catalytic dehydrogenation of hydrazine was achieved over iminopyridine ligated ruthenium-arene complexes, where the release of H_2 gas, as confirmed by GC-TCD, from hydrazine depends on reaction temperature, base, and solvents. NMR and mass studies evidenced the *in situ* generation of a hydrazine coordinated ruthenium species, a key intermediate of hydrazine dehydrogenation via a coordination assisted activation pathway.